Tunable band gap in a photonic crystal modulated by a nematic liquid crystal

Chen-Yang Liu and Lien-Wen Chen*
Department of Mechanical Engineering, National Cheng Kung University, Tainan 70101, Taiwan
(Received 17 August 2004; revised manuscript received 4 March 2005; published 20 July 2005)

Photonic crystals (PCs) have many potential applications because of their ability to control light-wave propagation. We have investigated the tunable band gap in a photonic crystal modulated by a nematic liquid crystal. Numerical simulations show that the band gaps can be continuously tuned in two-dimensional square and triangular lattices of cylinders by infiltrating nematic liquid crystals. Then we can control the band gap in a PC structure. We also analyzed the gap maps of tunable band gap by considering various indices modulation of liquid crystals. These results can be used as tunable field-sensitive polarizer in photonic integrated circuits.

DOI: 10.1103/PhysRevB.72.045133 PACS number(s): 42.70.Qs, 42.70.Df, 42.79.Ci

I. INTRODUCTION

Photonic crystals (PCs) are artificial dielectric or metallic structures in which the refractive index modulation gives rise to stop bands for optical waves within a certain frequency.[1,2] These crystals have many potential applications because of their ability to control light-wave propagation. The periodicity is broken by introduction of some defects into the crystals. It has been shown that doped PCs permit the guiding of waves in two different geometric paths for two distinct wavelength ranges.[3] Such structures can be use to design highly efficient optical devices. Optical waveguides in two-dimensional (2D) PCs produced by insertion of linear defects into PC structures had been proposed[4] and experimentally proved.[5] PCs had attracted much attention in the fabrication of high-Q microcavities. The introduction of a local defect inside a perfect 2D periodic dielectric structure may give rise to a sharp resonant state inside the crystal in the vicinity of the defect. Villeneuve *et al.* investigated the properties of a tunable single-mode waveguide microcavity that is well studied for frequency modulation and switching.[6,7] Planar PC circuits consist of devices, such as splitters,[8] filters,[9] and multichannel drop filters,[10] by controlling the interaction between static devices, such as waveguides, cavities, or horns. However, for many wavelength division multiplexing applications, it would prove advantageous to tune these devices, to some degree, to enable wavelength selectivity.

Recently, it was found that the anisotropy in atom dielectricity can break the degeneracy of photonic bands such that partial band gaps can be created in fcc, bcc, and simple cubic (sc) lattices.[11] It was also demonstrated that an anisotropy in dielectricity can remarkably increase absolute band gaps in 2D PC structures.[12,13] More recently, Kushwaha and Martinez were concerned with a 2D periodic system of semiconductor cylinders embedded in a dielectric background.[14]

It is important, however, to obtain tunable PC waveguides for applications in optical devices. Tunable PC waveguides that utilize synthetic opals and inverse opals infiltrated with functional materials have been proposed.[15,16] One can control the refractive indices of opals by adjusting various factors and fields. For example, one can change the refractive indices of conducting polymers and liquid crystals (LCs) by changing the temperature and the electric field of the polymer or crystal. Therefore one can change the optical properties of tunable PC waveguides composed of such materials by changing the temperature and the electric field in the same way. Recently, the propagation of tunable light in Y-shaped waveguides in 2D PCs by use of LCs as linear defects was proposed.[17,18] The tunable PC waveguide coupler based on nematic LCs was presented by the authors.[19]

In this paper, we theoretically demonstrated the tunable band gaps of transversal electric (TE) and transversal magnetic (TM) modes in 2D PC structure with nematic LCs. The 2D PC structures are assumed to be composed of Si circular rods with square or triangular lattices surrounded by the LC. The band gaps can be controlled by rotating directors of LCs under the influence of the applied electric field. We also presented a field-sensitive polarizer to explain how to use this tunable PC structure.

II. NUMERICAL METHOD

Following discussion of Busch and John,[20] we can express the light-wave equation that is satisfied by the magnetic field for 2D planes in order to determine the photonic bandgaps of 2D periodic structures utilizing nematic LCs

$$\nabla \times \left[\frac{1}{\varepsilon(r)} \nabla \times H(r) \right] = \left(\frac{\omega}{c} \right)^2 H(r), \tag{1}$$

where $\nabla H(r)=0$. The dielectric tensor $\varepsilon(r)=\varepsilon(r+R)$ is periodic with respect to lattice vector R generated by primitive translation, and it may be expanded in a Fourier series on $\mathbf{G}$, the reciprocal lattice vector as

$$\varepsilon_{ij}(r) = \sum_G \varepsilon_{ij}(\mathbf{G}) \exp(i\mathbf{G} \cdot r) \quad (i,j = x,y) \tag{2}$$

Generally LCs possess two kinds of dielectric index. One is ordinary dielectric index ε^o, and the other is extraordinary dielectric index ε^e. Light waves with electric fields perpendicular and parallel to the director of the LC have ordinary and extraordinary refractive indices, respectively. Extended Jones matrix method[21] is a simple and powerful approach for dealing with the light transmission problem of a LC device at normal incidence. In the 2D plane, the components of the dielectric tensor of the nematic LC are represented as

$$\varepsilon_{xx}(r) = \varepsilon^o(r)\sin^2\phi + \varepsilon^e(r)\cos^2\phi, \tag{3}$$

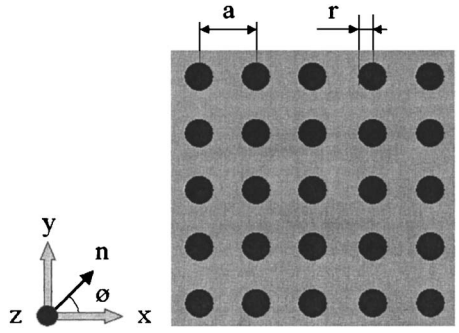

FIG. 1. Photonic crystal structure with square lattices. The shaded region is infiltrated with liquid crystals. The left inset indicates the director of a liquid crystal.

$$\varepsilon_{yy}(r) = \varepsilon^o(r)\cos^2\phi + \varepsilon^e(r)\sin^2\phi, \tag{4}$$

$$\varepsilon_{xy}(r) = \varepsilon_{yx}(r) = [\varepsilon^e(r) - \varepsilon^o(r)]\cos\phi\sin\phi, \tag{5}$$

where ϕ is the rotation angle of the director of the LCs and $n=(\cos\phi, \sin\phi)$ is the director of the LC, as shown in Fig. 1.

Equation (1) comprises a set of three coupled differential equations with periodic coefficients. We define $e_{\mathbf{G}}$ as the direction that is perpendicular to the 2D plane. Using Bloch's theorem, we may expand the magnetic field as

$$H(r) = \sum_{\mathbf{G}} h(G)e_{\mathbf{G}}\exp[i(k+\mathbf{G})\cdot r]. \tag{6}$$

We could insert Eq. (2)–(6) into Eq. (1) and multiply by the $e_{\mathbf{G}}$ result in the following infinite matrix eigenvalue problem:

$$\sum_{\mathbf{G}'} H_{\mathbf{G},\mathbf{G}'}h(\mathbf{G}') = \left(\frac{\omega}{c}\right)^2 h(\mathbf{G}). \tag{7}$$

We assume the TE and TM modes in the cases of director of LCs parallel and perpendicular to 2D planes. The main numerical problem in obtaining the eigenvalue is the evaluation of the Fourier coefficients of the inverse dielectric tensors. The best method is to calculate the matrix of Fourier coefficients of real-space tensors and take its inverse in order to obtain the required Fourier coefficients. This method was shown by Ho *et al.* (HCS).[22] The eigenvalues computed with the HCS method for 441 plane waves are estimated to be in error $<1\%$.

The ordinary and extraordinary refractive indices of liquid crystals (5CB type) are $n^o_{LC}=1.522$ and $n^e_{LC}=1.706$, respectively. The inset in Fig. 1 indicates the director n of a liquid crystal and the rotation angle ϕ of the director to the x axis. The mesogenic temperature range of a single LC substance is usually quite limited.[21] For example, 5CB melts at 24 °C and clears at 35.3 °C. 5CB is a nice material to work with because it exhibits a nematic phase at room temperature and its nematic range is $>10°$. We assume that the operating temperature is at a constant room temperature and that the absorption loss is negligible.

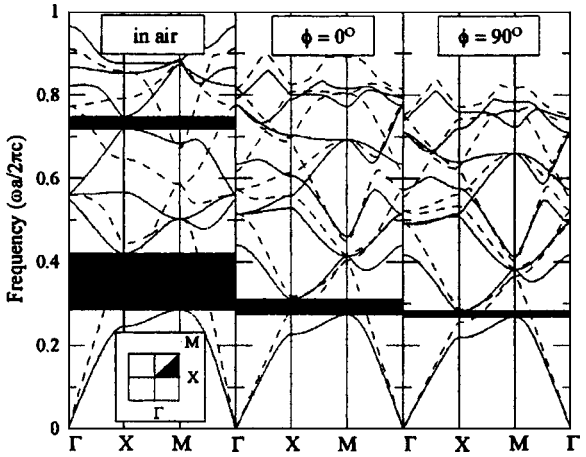

FIG. 2. Calculated photonic band structures of the 2D square array of Si cylinders for TM mode (solid line) and TE mode (dotted lines) in the air (left), in the nematic liquid crystal at $\phi=0°$ (center), and in the nematic liquid crystal at $\phi=90°$ (right). The radius of cylinders is taken as $r=0.2a$. The hatched areas represent photonic band gaps for TM mode.

III. PC SURROUNDED BY LC

We consider that a 2D PC composed of square-lattice dielectric cylinders surrounded by LC 5CB, as shown in Fig. 1. The lattice constant is a and the radius of cylinders is r. The refractive index of cylinders is taken as $n_0=3.4$ (Si). The material is homogeneous in the z direction and periodic along x and y with lattice constant. In Fig. 2, we show the photonic band structures of 2D square lattice of dielectric cylinders in the air (left), in the nematic liquid crystal at $\phi=0°$ (center), and in the nematic liquid crystal at $\phi=90°$ (right), respectively. We have chosen $r=0.2a$, since the 2D square lattice of cylinders in the air shows the largest bandgap for TM mode. The perfect PC structure in air has two band gaps for TM mode. One is a large band gap between the first and second bands ($\omega a/2\pi c=0.2856$–0.4207), and the other is a small band gap between the fourth and fifth bands ($\omega a/2\pi c=0.7191$–0.7480), where ω is the angular frequency and c is the light velocity in the free space. It is also clear that the infiltration of LC makes the second band gap disappear and the upper edge of the first band gap moves down drastically with little decrease of bottom edge. The infiltration of LC can shift the band gap to 0.2737–0.3109 at $\phi=0°$ and 0.2685–0.2819 at $\phi=90°$.

The gap maps for a square lattice of dielectric cylinders are shown in Fig. 3. At a glance, the gap map reveals some interesting regularities. First, the gaps all decrease in frequency as r/a increases. Second, the gaps all decrease in frequency as ϕ increases. The third, the gaps at higher frequencies disappear as ϕ increases. The fourth, all of the gaps seal up at $r/a=0.5$. At that value, the dielectric cylinders begin to touch one another. The dielectric cylinders fill space at $r/a=0.7$. The fifth, there are no significant TE gaps at all for square lattice in the frequency range displayed. The results mean that the bandgaps of PCs can be actively modulated by infiltrating nematic LCs.

Such a concept is also applicable to other lattice types and atom configurations. We consider that a 2D PC composed of

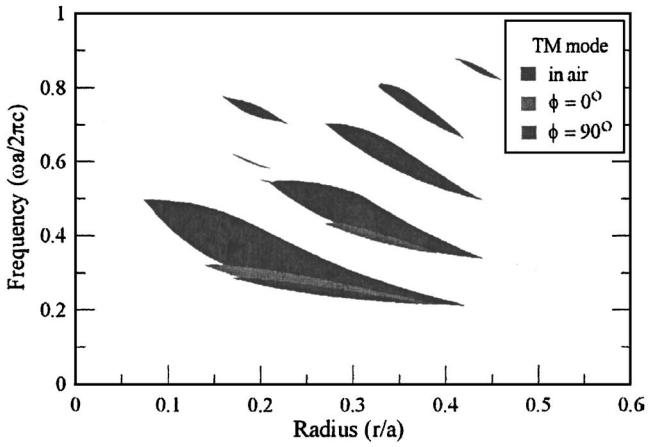

FIG. 3. (Color online) Gap maps for a square lattice of dielectric cylinders.

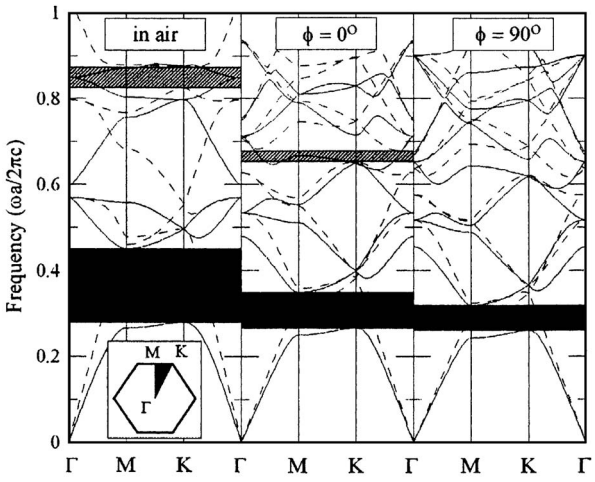

FIG. 4. Calculated photonic band structures of the 2D triangular array of Si cylinders for TM mode (solid line) and TE mode (dotted lines) in the air (left), in the nematic liquid crystal at $\phi=0°$ (center), and in the nematic liquid crystal at $\phi=90°$ (right). The radius of cylinders is taken as $r=0.2a$. The hatched areas represent photonic bandgaps for TM mode (gray region) and TE mode (crosshatched region).

triangular-lattice dielectric cylinders surrounded by LC 5CB. We calculated the photonic band structure of 2D triangular arrays using the same parameters as those employed in the square lattice. In Fig. 4, we show the photonic band structures of 2D triangular lattice of dielectric cylinders in the air (left), in the nematic liquid crystal at $\phi=0°$ (center), and in the nematic liquid crystal at $\phi=90°$ (right). The perfect PC structure in air has two photonic band gaps for TM and TE modes, respectively. One is a large band gap between the first and second bands ($\omega a/2\pi c=0.2792$–0.4501) for TM mode, and the other is a small one between the fourth and fifth bands ($\omega a/2\pi c=0.8251$–0.8738) for TE mode. It is also clear that the infiltration of LC makes the band gaps for TM and TE modes shifted to 0.2661–0.3488 and 0.6525–0.6789 at $\phi=0°$. We can see from Fig. 4 that the band gap shifted to 0.2602–0.3189 at $\phi=90°$ for TM mode, and disappeared at $\phi=90°$ for TE mode.

The gap maps for a triangular lattice of dielectric cylinders are shown in Fig. 5. The remarkable self-similarity of Fig. 3, which was for TM mode of the square lattice of dielectric cylinders, is mirrored here. The successive gaps are similar in shape and orientation, and stack regularly upon one another. The dielectric cylinders begin touching one another at $r/a=0.5$ and fill space at $r/a=0.58$. The cutoff at $r/a=0.45$ is once again near the cylinder-touching condition. The gap maps for TE mode is almost as sparse as the corresponding case of the square lattice. Only a few slivers are noticeable. The gaps decrease in frequency as ϕ increases.

Figure 6 shows the variation of band gap due to the change of the rotation angle of LC. The colored areas represent tunable band gaps. They all decrease in frequency as ϕ increases. The band gap of the triangular lattice for TE mode sealed up at $\phi=70°$. The results show that the band gaps could be actively modulated after infiltrating nematic LCs. This tunable PC can act as a tunable planar lightwave component. An example of tunable field-sensitive polarizer design is discussed in Sec. IV.

IV. TUNABLE FIELD-SENSITIVE POLARIZER

We see then that the band gap can be continuously tuned by relatively electric fields. This tunable PC can act as a

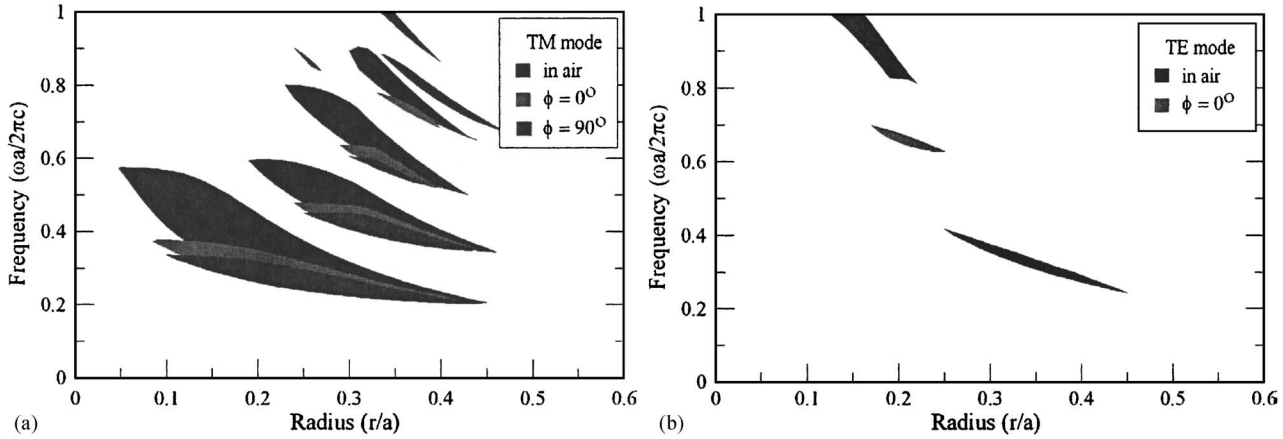

FIG. 5. (Color online) Gap maps for a triangular lattice of dielectric cylinders.

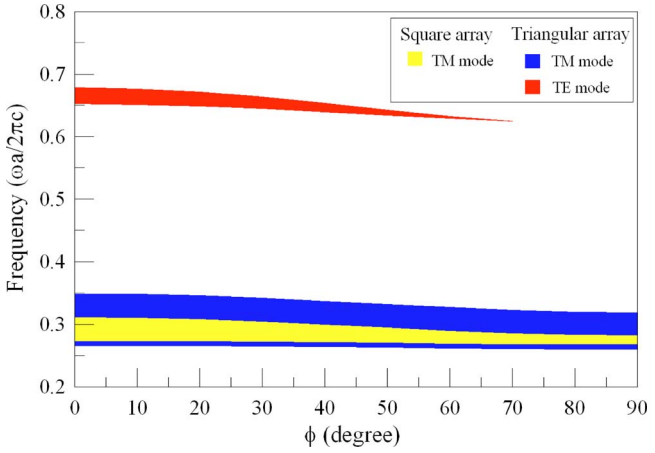

FIG. 6. (Color online) Photonic bandgap as a function of rotation angle ϕ. The radius of cylinders is taken as $r=0.2a$. The colored areas represent photonic band gaps.

field-sensitive polarizer. For example, unpolarized light of frequency $\omega a/(2\pi c)=0.34$ will be transmitted if $\phi=90°$; however, only the TE-polarized component will be transmitted if $\phi=0°$, as can be seen from Fig. 6. This is because there is no complete band gap for the TE mode.

We propose the hybrid integration of conventional index-guided waveguides and PC structure with LC. The schematic model of tunable planar field-sensitive polarizer is shown in Fig. 7. The conventional waveguide has core and clad refractive indices of $n_1=1.5$ and $n_2=1.465$, respectively. The conventional waveguide has a width of 2 μm so it supports a single-guided mode for wavelength in the telecommunication band near 1.55 μm. The PC lattice is composed of a triangular array of silicon posts with a lattice constant $a=500$ nm, and a post radius $r=0.2a$.

In nematic LCs the directors of the LCs depend on the direction of the electric field in 2D planes. Indium tin oxide (ITO) layers can be attached to the top and bottom of the PC structure. Then we can apply the electric field that sums up the electric fields in the x and the y directions in arbitrary directions in 2D planes by adjusting the magnitudes of the electric field in the x and y directions, respectively, making it possible to rotate the directors of the LCs. Figure 8 shows the computer simulations of the rotation angle ϕ as a function of normalized voltage. The director can be reoriented by an electric field when the field strength exceeds the Fréedericksz transition threshold.[21] When the applied voltage V exceeds the Fréedericksz transition threshold (V_{th}), the directors begin to tilt. V_{th} is the threshold voltage that is found to be 0.699 V_{rms} at 1 kHz sinusoidal frequency. Figure 9 shows the computer simulations of the band gap as a function of normalized voltage. The applied electric field is in the small voltage region. The colored areas represent tunable band gaps. The band gaps decrease in frequency as applied voltage increases.

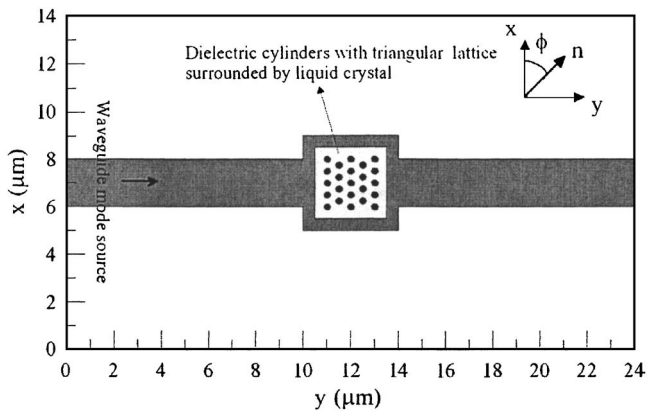

FIG. 7. A tunable field-sensitive polarizer constructed with hybrid conventional waveguide and PC structures.

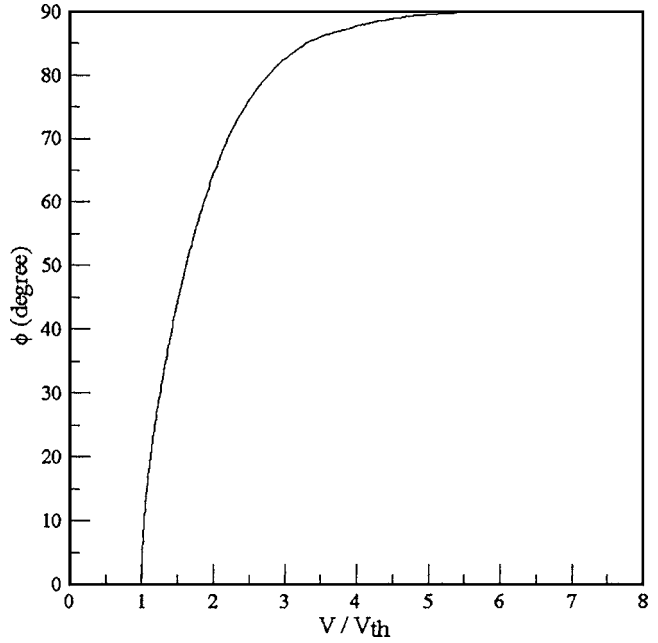

FIG. 8. Calculated rotation angle ϕ as a function of normalized voltage. V_{th} is the threshold voltage.

In general, the response time of a LC is of the order of a millisecond. However, it has been reported that the response time of LCs in nanoscale voids becomes of the order of 100 μs.[23] The orientational relaxation times calculated by

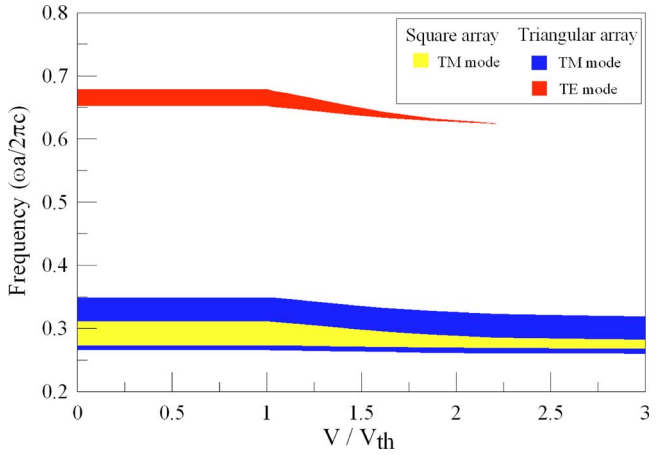

FIG. 9. (Color online) Calculated photonic band gap as a function of normalized voltage. The applied electric field is in the small voltage region. The radius of cylinders is taken as $r=0.2a$. The colored areas represent tunable band gaps.

the molecular dynamics formalism, and the experimental data determined by nuclear magnetic resonance spectroscopy for the nematic phase of 5CB crystal at 300 K were presented in Ref. 24. Therefore our tunable PC structure with LCs can be used as a fast field-sensitive polarizer in planar photonic integrated circuits.

V. CONCLUSION

We have demonstrated, numerically, from the photonic band calculation, the effects of LC infiltration on the band gaps of 2D square and triangular lattices of dielectric cylinders. It is also demonstrated that the band gap can be controlled by rotating directors of LCs under the influence of applied electric field. We analyzed the gap maps by considering various indices modulation of liquid crystals. Because of large varieties of anisotropic materials in LC, this opens up a scope for designing the tunable devices in photonic integrated circuits. Further theoretical investigations and many experimental efforts are needed to bring the tunable band gap into reality.

*E-mail: chenlw@mail.ncku.edu.tw

[1] E. Yablonovitch, Phys. Rev. Lett. **58**, 2059-2062 (1987).
[2] J. D. Joannopoulos, R. D. Mead, and J. N. Winn, *Photonic Crystal* (Princeton University Press, Princeton, NJ, 1995).
[3] E. Centeno and D. Felbacq, Opt. Commun. **160**, 57-60 (1999).
[4] R. D. Meade, A. Devenyi, J. D. Joannopoulos, O. L. Alerhand, D. A. Smith, and K. Kash, J. Appl. Phys. **75**, 4753-4755 (1994).
[5] T. Baba, N. Fukaya, and J. Yonekura, Electron. Lett. **35**, 654-656 (1999).
[6] P. R. Villeneuve, D. S. Abrams, S. Fan, and J. D. Joannopoulos, Opt. Lett. **21**, 2017-2019 (1996).
[7] P. R. Villeneuve, S. Fan, and J. D. Joannopoulos, Phys. Rev. B **54**, 7837-7842 (1996).
[8] S. Fan, S. G. Johnson, J. D. Joannopoulos, C. Manolatou, and H. A. Haus, J. Opt. Soc. Am. B **18**, 162-165 (2001).
[9] R. Costa, A. Melloni, and M. Martinelli, IEEE Photonics Technol. Lett. **15**, 401-403 (2003).
[10] A. Sharkawy, S. Shi, and D. W. Prather, Appl. Opt. **40**, 2247-2252 (2001).
[11] Z.-Y. Li, J. Wang, and B.-Y. Gu, Phys. Rev. B **58**, 3721 (1998).
[12] Z.-Y. Li, B.-Y. Gu, and G.-Z. Yang, Phys. Rev. Lett. **81**, 2574 (1998).
[13] Z.-Y. Li, B.-Y. Gu, and G.-Z. Yang, Eur. Phys. J. B **11**, 65 (1999).
[14] M. S. Kushwaha and G. Martinez, Phys. Rev. B **65**, 153202 (2002).
[15] K. Yoshino, Y. Shimoda, Y. Kawagishi, K. Nakayama, and M. Ozaki, Appl. Phys. Lett. **75**, 932-934 (1999).
[16] H. Takeda and K. Yoshino, J. Appl. Phys. **92**, 5958-5662 (2002).
[17] H. Takeda and K. Yoshino, Phys. Rev. B **67**, 073106 (2003).
[18] H. Takeda and K. Yoshino, Opt. Commun. **219**, 177-182 (2003).
[19] C.-Y. Liu and L.-W. Chen, IEEE Photonics Technol. Lett. **16**, 1849-1851 (2004).
[20] K. Busch and S. John, Phys. Rev. E **58**, 3896 (1998).
[21] I.-C. Khoo, and S.-T. Wu, *Optics and Nonlinear Optics of Liquid Crystals* (World Scientific, Singapore, 1993).
[22] K. M. Ho, C. T. Chan, and C. M. Soukoulis, Phys. Rev. Lett. **65**, 3152-3155 (1990).
[23] Y. Shimoda, M. Ozaki, and K. Yoshino, Appl. Phys. Lett. **79**, 3627-3629 (2001).
[24] A. V. Zakharov and L. V. Mirantsev, Phys. Solid State **45**, 183-188 (2003).